



**24th COBEM - 2017**



24th ABCM International Congress of Mechanical Engineering  
December 3-8, 2017, Curitiba, PR, Brazil

**COBEM-2017-2873**

## **AN EXPERIMENTAL STUDY ON THE IMPACT BEHAVIOR OF CF/EPOXY CIRCULAR TUBES**

**Pouria B. Atabadi**

University de São Paulo, Group of Solid Mechanics and Structural Impact, São Paulo, Brazil  
Pouriabahrami@usp.br

**D. Karagiozova**

Institute of Mechanics, Bulgarian Academy of Sciences, Sofia, Bulgaria  
D.karagiozova@gmail.com

**L. Driemeier**

University de São Paulo, Group of Solid Mechanics and Structural Impact, São Paulo, Brazil  
Driemeie@usp.br

**M. Alves**

University de São Paulo, Group of Solid Mechanics and Structural Impact, São Paulo, Brazil  
Maralves@usp.br

**Abstract.** *Quasi-static and impact tests on carbon fiber – epoxy tubes were carried out in order to reveal the effect of the loading parameters- striking mass and impact velocity- on their deformation mechanisms. The crushing behavior and energy absorption capacity of circular CF/Epoxy tubes were investigated. Tubes with two different stacking sequences were used in the quasi-static and impact tests and the effects of fiber orientation and loading rates on the crushing modes and SEA (Specific Energy Absorption) of the tubes were explored, with the results being compared and discussed. The experimental results show that the crushing modes of tubes under quasi-static and dynamic crushing are stacking sequence dependent which lead to a difference in their energy absorption capacity. The influence of the shape of chamfer, which was used as a crushing trigger, on the peak load was also analyzed.*

**Keywords:** *Carbon fiber composites, Circular tube, quasi-static compression, dynamic axial crushing.*

### **1. INTRODUCTION**

Nowadays, with the growing concern with the environmental issues and fuel price increase, the major car and aircraft producing companies have been motivated to incorporate advanced composite materials with high specific strength and specific stiffness ratios into their products. At the beginning, these companies were mainly concerned with the weight optimization by replacing same metallic parts with lighter materials without scarifying the general safety level of the vehicles, however, later the superior energy absorption behavior of the composite materials encouraged the designers to substitute especially designed metallic absorber by composite ones which exhibit a more desirable performance in terms of the load-displacement response as illustrated in Fig.1.

A laminated composite tube can fail by two general failure modes; (i) progressive crushing modes, for example ‘splaying mode’, ‘fragmentation mode’ and ‘brittle fracturing mode’, and (ii) catastrophic modes, for example Euler buckling (Hull, 1991). In fact, the aim of crashworthy design is to prevent catastrophic modes and control the progressive crushing to achieve higher absorbed energy. The progressive modes include a combination of inter-laminar failure, delamination, and intra-laminar failure such as fiber breakage, matrix crack, fiber–matrix debond, lamina bundle bending etc. There are many parameters affecting inter-laminar and intra-laminar mechanical properties of laminated composites that control energy absorption and crush zone presentation of laminate composite structures, therefore, the design and analysis processes are more complicated than metallic structural members, so it is possible to design energy absorbers with better tailored characteristics when using composite materials.

The analysis of the energy absorption capacity of Carbon Fiber Reinforced Plastics (CFRPs) structural members is gaining increasing attention in the crashworthy design. In particular, the energy absorption capacity of circular CFRP tubes, as a substitution for metallic ones, has been investigated by several researchers and still is an ongoing trend

among engineers around the world (Schultz and Hyer, 2001; Wade, 2014; Wang, et al., 2016). Despite the fact that there is a considerable number of publications on the energy absorption capacity of CFRPs, the current insight into their behavior under dynamic loading is less well understood in comparison with the behavior of dynamically loaded metallic tubes.

The parameters which influence the energy absorption capacity of tubular composites are (i) testing speed (Farley, 1983; Mamalis, et al., 1986; Snowdon and Hull, 1984; Bannerman and Kindervater, 1984; Scueser and Wickliffe, 1987; Russell, et al., 1991; Thornton, 1990), (ii) geometric parameters (Farley, 1983; Farley, 1987; Chadwick and Caliskan, 1997; Fairfull and Hull, 1987), (iii) trigger mechanism (Farley, 1983; Grundy, et al., 1985; Soica and Radu, 2013) and (iv) stacking sequence of lamination (Hull, 1991; Hamouda and Sebaey, 2014). Although consistent conclusions about the influence of these parameters on the crashworthiness of composite materials were reported, some contradictory observations were made. For instance, most of the researchers have reported a decrease of the SEA value (Scueser and Wickliffe, 1987; Russell, et al., 1991; Thornton, 1990) when increasing the crushing speed while others reported an increase (Bannerman and Kindervater, 1984) or no change or very little change (Farley, 1983; Mamalis, et al., 1986; Snowdon and Hull, 1984) in the SEA values. The similar issue can be noticed for other investigated parameters. These apparent contradictions emphasize on the lack of a standardized test method to characterize the energy absorption capability of a composite material system because its energy absorbing mechanisms are still not well understood (Wade, 2014).

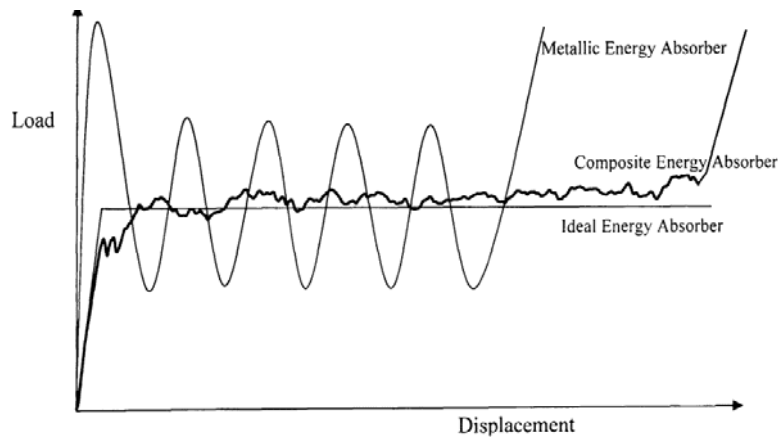


Figure 1. Metallic and composite absorber behaviors in comparison with an ideal absorber.

As the investigation on the energy absorption of CFRPs is still an interesting and challenging issue in the crashworthy design field, in the present work the kinetic energy absorption capacity of Carbon/Epoxy tubes under axial quasi-static compression and dynamic crushing is experimentally investigated. Moreover, the effects of stacking sequence and trigger mechanism on the absorbed energy were experimentally studied and compared with previous finding available in the literature.

To investigate the crashworthiness of materials and structures, some valuation criteria are required. The most common criteria to qualify the performance of kinematic energy absorbers are the Specific Energy Absorption (SEA), Crush Force Efficiency (CE), peak force ( $F_{peak}$ ) and average crushing load ( $F_{ave}$ ), (Jones, 1993). The load-displacement curve of the structural member is commonly used in crashworthy design to obtain the values of the above characteristics. The area under load-displacement curve is equal to the absorbed energy, SEA is calculated when dividing this energy by mass of crushed part of the structure. Table 1 presents formulas for calculating these valuation criteria, where  $F$  is the crushing load,  $m_l$  is mass per unit length of the tube and  $l_f$  is final crushed length of tube.

Table 1. The valuation criteria in the crashworthy design, (Jones, 1993).

Criterion	Symbol	Unit	Definition
Absorbed energy	AE	J	$E_A = \int_0^{l_f} F dl$
Mass of crushed part	$m_c$	g	$m_c = m_l l_f$
Average crushing load	$F_{ave}$	N	$F_{ave} = AE / l_f$
Crush efficiency	CE	-	$CE = F_{ave} / F_{peak}$
Specific Energy Absorption	SEA	J/g	$SEA = AE / m_c$

## 2. EXPERIMENTAL PROCEDURE

### 2.1 DESCRIPTION OF SPECIMENS

In the present work, there are two different families of circular tubes with different stacking sequences under investigation. These two stacking sequences given in Table 2 are selected to investigate the effects of ply orientations on the energy absorption capacity of laminated CFRPs. The internal diameters and thicknesses of both tubes were chosen equal in order to minimize the effect of cross-section area when comparing the energy absorption of two different tubes configurations. In the tubing process the prepreg materials were wrapped around a mandrel having 50 mm outer diameter then curing process had been done into an autoclave. The mechanical properties of laminae are presented in Table 3.

In the present work specimens were chamfered externally with different angles at only one end, as depicted in Fig. 2. Tubes with chamfer angles,  $\theta$ , equal to 45 and 60 degrees were tested to investigate the effect of this triggering mechanism on energy absorption characterization of carbon fiber tubes. Furthermore, tubes with square ends (without any crash initiator) were impacted to reach a better insight into roles of trigger mechanism.

Table 2. Description of tubes.

Item	Tube configuration #1	Tube configuration #2
Stacking sequence <sup>(1)</sup>	$[\pm 45/0/\pm 45/0/\pm 45/0/\pm 45]$	$[0/(90)_2/0]_s$
Inner diameter (mm)	50.00	50.00
Thickness (mm)	2.24	2.20

<sup>(1)</sup> 0,  $\pm 45$  and 90 are measured from tube axis, as introduced in Fig. 2 with  $\varphi$ .

Table 3. Nominal mechanical properties of CF/Epoxy laminae.

Property	Symbol	Units	UD <sup>(1)</sup>
Elastic modulus 0°	$E_1$	GPa	135
Elastic modulus 90°	$E_2$	GPa	10
In-plane shear modulus	$G_{12}$	GPa	5
Major Poisson's ratio	$\nu_{12}$	-	0.3
Ultimate tensile strength 0°	$S_{1t}$	MPa	1500
Ultimate tensile strength 90°	$S_{2t}$	MPa	50
Ultimate compressive strength 0°	$S_{1c}$	MPa	1200
Ultimate compressive strength 90°	$S_{2c}$	MPa	250
Shear Strength	S	MPa	70

<sup>(1)</sup> Unidirectional layers' thicknesses are equal to 0.3 or 0.2 mm.

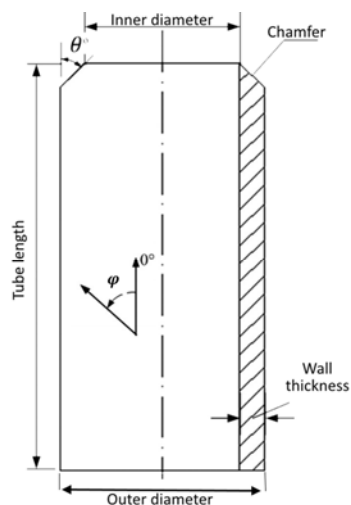


Figure 2. Tubular specimen schematic presentation including chamfer, wall thickness, ID and OD.

### 2.2 DESCRIPTION OF AXIAL QUASI-STATIC COMPRESSION TESTS AND RESULTS

The static tests were carried out on an Instron 3369 and MTS machines at the University of São Paulo. Figure 3 presents the static tests setup where the specimen is placed on the stationary platen of the machine. The cross-head speed was set at 0.5 mm per minute and the cross-head is lowered until the upper platen was just touching the specimen. The cross-head was then set into motion meanwhile the load and cross-head displacement were recorded for each test. Finally, the raw data was used to find some crashworthy criteria defined in Table 1. Photos of crush mode of each specimen were taken after test.

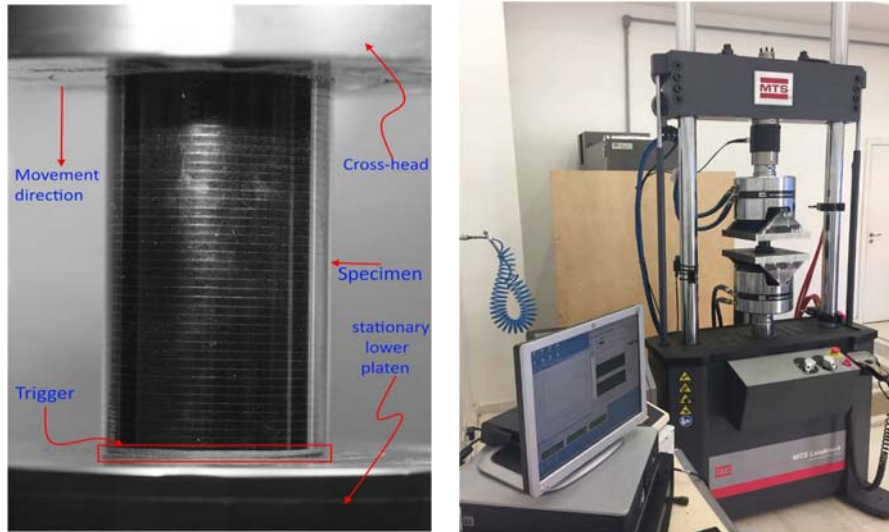


Figure 3. The quasi-static test setup.

The dimensions and performance of specimens under quasi-static compression tests in the present study are presented in Table 4.

Table 4. Dimensions and results of specimens under quasi-static compression.

Specimen ID	Trigger ( $\theta$ )	Stacking sequence	Crushed length (mm)	Mass/length (g/mm)	$F_{Peak}$ (KN)	$F_{ave}$ (KN)	SEA (J/g)	CE
AS45#1.a	45	[ $\pm 45/0...$ ]	67.99	0.595	43.67	36.52	61.35	0.83
AS45#1.b	45	[ $\pm 45/0...$ ]	65.58	0.589	47.77	37.64	63.86	0.78
AS60#2.a	60	[ $\pm 45/0...$ ]	58.35	0.595	58.96	32.29	54.19	0.54
AS60#2.b	60	[ $\pm 45/0...$ ]	75.01	0.589	53.17	33.11	56.17	0.62
AS00#3.a	0	[ $\pm 45/0...$ ]	50.76	0.593	78.26	40.31	67.95	0.51
AS00#3.b	0	[ $\pm 45/0...$ ]	74.98	0.592	90.71	40.47	68.37	0.44
CS00#4.a	0	[0/90...]	69.99	0.541	68.23	32.37	59.85	0.47
CS00#4.b	0	[0/90...]	70.01	0.538	66.31	30.85	57.36	0.46
CS60#5.a	60	[0/90...]	65.39	0.544	47.32	30.46	56.80	0.64
CS60#5.b	60	[0/90...]	66.01	0.543	44.88	31.49	57.60	0.70
CS45#6.a	45	[0/90...]	60.13	0.536	39.18	30.35	55.73	0.77
CS45#6.b	45	[0/90...]	77.42	0.548	39.41	31.65	58.20	0.80

### 2.3 DYNAMIC CRUSHING TESTS DESCRIPTION AND RESULTS

The drop tower facility at GMSIE Laboratory at the University of Sao Paulo shown in Fig. 4 was used to perform axial dynamic impacting tests. The striker weight can be increased up to one tone and maximum obtainable height of striker mass is about 9 meter that approximately will provide 13.2 m/s impact speed. The specimen was placed on the base of drop tower freely (without using any glue or fixture) and the striker was raised to a suitable height to give the desired impact velocity. To start the test, the striker was released and the specimen was impacted by the striker mass. Laser velocity meter and ADC unit were used to measure and record the velocity of the striker for further required calculations. Besides, a high-speed camera was used to record the images during the test. At the end of each test, the final height of the specimen was measured. The recorded velocity was used to obtain the acceleration and crushing

force of the tubes. In this work tubes were impacted under two sets of dynamic crushing conditions; in set#1 the striker of 102 (Kg) had impacted the specimens with initial velocity of 5 (m/s), in the set#2 the mass of striker is increased to 205 (Kg) and it had crushed the specimens with initial velocity of 5 (m/s). Specimens' dimensions and their performance under different dynamic crushing conditions are presented in Tables 5-6.

Recorded signal by the laser velocity meter was filtered by using different available filter in MATLAB, such as Butterworth and smooth function (a moving average filter), then acceleration of striker is derived from its filtered velocity. The crushing load of dynamic tests is calculated by using the following formula.

$$\text{Crash force} = mg + m \frac{dV}{dt} \quad (1)$$

where  $g$  is gravity acceleration,  $m$  and  $V$  are the mass and velocity of striker, respectively.

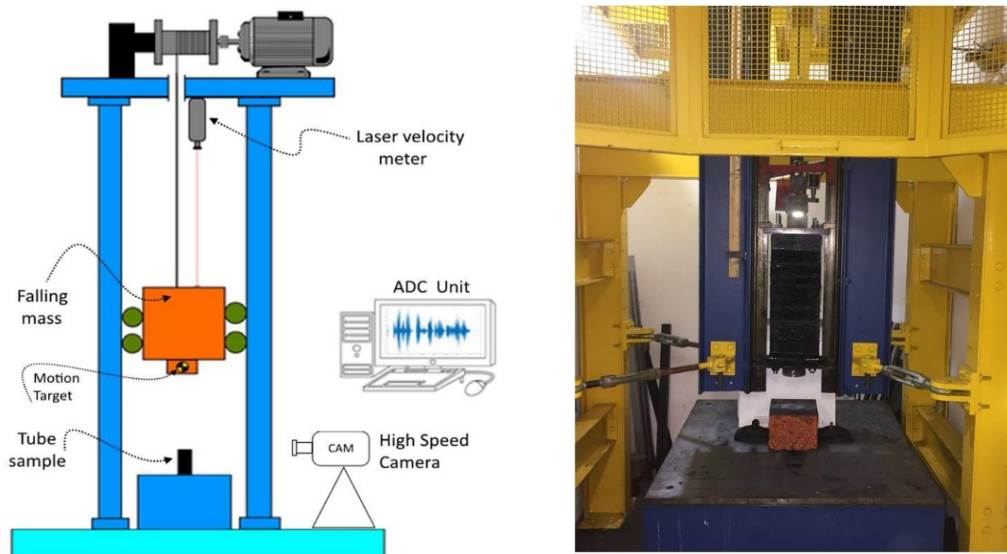


Figure 4. Drop tower facility at GMSIE Laboratory.

Table 5. Specimens dimensions and their performance under dynamic crushing, set#1.

Dynamic tests: Set#1								
Nominal velocity = 5 (m/s)								
Striker mass = 102 (kg)								
Nominal kinetic energy = 1275 (J)								
Specimen ID	Stacking sequence	Trigger ( $\theta$ )	$E_K$ (kJ) <sup>(1,2)</sup>	$E_A$ (kJ) <sup>(3)</sup>	Crushed length (mm)	SEA (J/g)	$F_{ave}$ (KN)	Mass per length (g/mm)
AD45#7.a	[±45/0..]	45	1.341	1.293	37.50	58.13	34.40	0.593
AD45#7.b	[±45/0..]	45	1.328	1.299	36.84	59.54	35.22	0.592
AD60#8.a	[±45/0..]	60	1.347	1.278	39.26	55.14	33.24	0.590
AD60#8.b	[±45/0..]	60	1.325	1.301	42.25	52.02	30.80	0.592
AD00#9.a	[±45/0..]	0	1.338	1.327	42.17	53.19	31.52	0.596
AD00#9.b	[±45/0..]	0	1.337	1.304	40.06	54.72	32.57	0.591
CD00#10.a	[0/90...]	0	1.326	1.310	44.39	54.20	29.31	0.542
CD00#10.b	[0/90...]	0	1.342	1.316	39.08	62.13	33.60	0.545
CD60#11.a	[0/90...]	60	1.316	1.217	35.62	62.98	31.50	0.543
CD60#11.b	[0/90...]	60	1.336	1.298	42.03	56.98	36.20	0.544
CD45#12.a	[0/90...]	45	1.326	1.298	43.33	55.52	30.02	0.545
CD45#12.b	[0/90...]	45	1.345	1.332	44.67	55.03	29.44	0.542

<sup>(1)</sup>  $E_K$ : Kinetic energy at impact initiation.

<sup>(2)</sup> The difference between nominal kinetic energy and actual kinetic energy is about 1%.

<sup>(3)</sup>  $E_A$ : Energy absorbed by specimen.

Table 6. Specimens dimensions and their performance under dynamic crushing, set#2.

Dynamic tests: Set#2								
Nominal velocity = 5 (m/s)								
Striker mass = 205 (KG)								
Nominal kinetic energy = 2562.50 (J)								
Specimen ID	Stacking sequence	Trigger ( $\theta$ )	$E_K$ (kJ) <sup>(1)</sup>	$E_A$ (KJ)	Crushed length (mm)	SEA (J/g)	$F_{ave}$ (KN)	Mass per length (g/mm)
AD45#13.a	[±45/0...]	45	2.732	2.631	83.18	53.47	31.5	0.591
AD45#13.b	[±45/0...]	45	2.741	2.632	92.97	47.74	28.0	0.592
AD60#14.a	[±45/0...]	60	2.709	2.643	90.19	49.53	29.1	0.591
AD60#14.b	[±45/0...]	60	2.702	2.635	83.59	53.21	31.4	0.592
AD00#15.a	[±45/0...]	0	2.761	2.628	96.80	45.88	27.1	0.591
AD00#15.b	[±45/0...]	0	2.701	2.575	92.23	47.25	27.9	0.591
CD00#16.a	[0/90...]	0	2.730	2.619	91.80	52.76	28.4	0.540
CD00#16.b	[0/90...]	0	2.713	2.596	89.90	53.24	28.8	0.542
CD60#17.a	[0/90...]	60	2.694	2.618	93.10	52.05	28.3	0.540
CD60#17.b	[0/90...]	60	2.704	2.588	93.84	50.7	27.5	0.541
CD45#18.a	[0/90...]	45	2.718	2.581	96.51	49.31	26.7	0.542
CD45#18.b	[0/90...]	45	2.747	2.632	94.06	51.58	27.9	0.542

<sup>(1)</sup>The difference between nominal kinetic energy and actual kinetic energy is about 8%.

### 3. DISCUSSION ON THE RESULTS

For all specimens, tests had been repeated at least 2 times (for example AD60#14.a and AD60#14.b). A good constancy between results is obvious. For dynamic tests the difference between kinetic energy,  $E_k$  and absorbed energy,  $E_A$  is lower than 9% which is reliable and can be related to the friction between striker and guides of hammer or other sources of energy losses. Moreover, all specimens, even specimens without trigger mechanism, had experienced a progressive crushing and catastrophic failure modes had not been observed in this study. Here, load-displacement response, crushing modes, SEA,  $F_{Peak}$ ,  $F_{ave}$  for quasi-static and dynamic impacting are presented and compared together.

#### 3.1 LOAD-DISPLACEMENT RESPONSE

The typical load-displacement curves of quasi-static compression for the two investigated stacking sequences are presented in Fig. 5. It is obvious that the ply orientation has a significant effect on the general shape of crushing force. Small fluctuations of the load-displacement curve of specimens with [0/90...] stacking sequence around its average value is observed while fluctuations with a larger magnitude characterize the crushing load of specimens with [±45/0...] stacking sequence.

Figure 6 shows and compares the typical force-displacement curves for two studied stacking sequences loaded dynamically. The behavior of the crushing force for [0/90...] and [±45/0...] lay-ups is similar in contract to the quasi-static compression of these tubes.

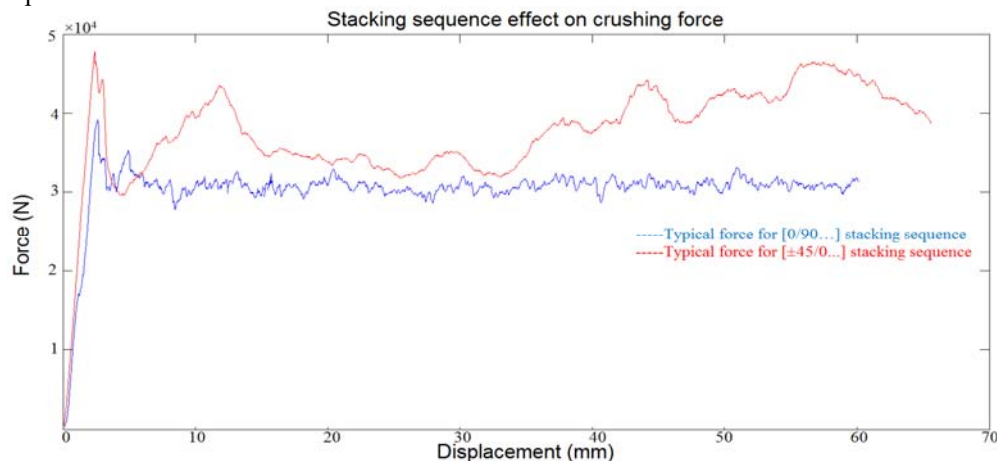


Figure 5. Typical load-displacement curve of specimens with different stacking sequences under quasi-static tests; red is related to AS45#1.b and blue is for CS45#6.a.

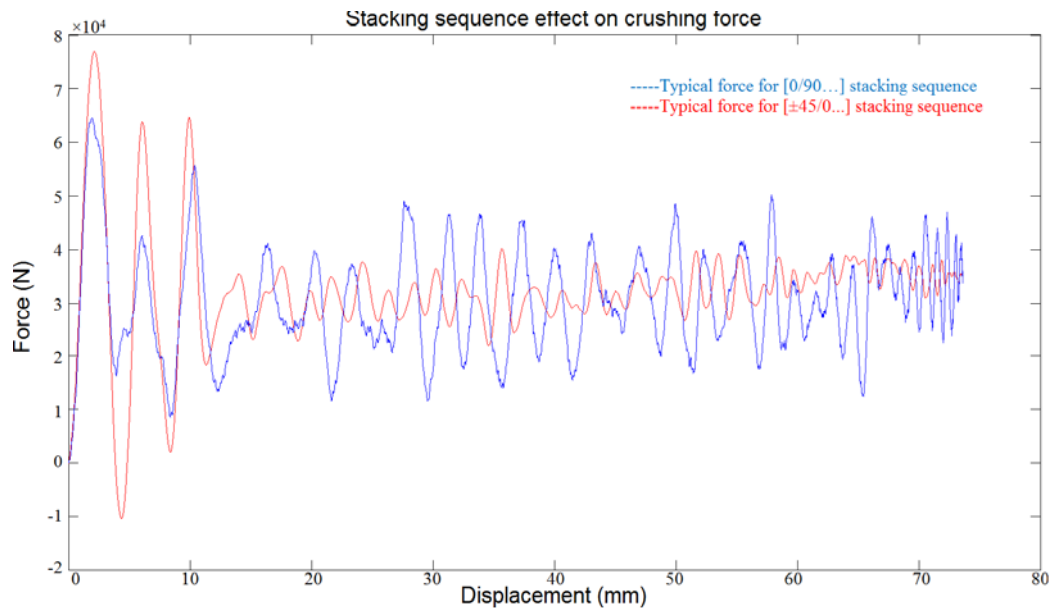


Figure 6. Typical load-displacement curve of specimens with different stacking sequences under dynamic tests.

### 3.2 PEAK LOAD, $F_{Peak}$

The peak load is a critical parameter in crashworthy design and there are several criteria for maximum allowable load that can be transmitted to the occupants without any injury. The peak load value of a tubular absorber under axial loading can be affected by cross-section area, trigger mechanism, ply orientation and loading rate. The cross-section areas of investigated tubes are approximately equal, thus, effects of other parameters on the peak load are presented as follows.

The specimens with  $[\pm 45/0...]$  stacking sequence had experienced higher peak loads comparing to those having  $[0/90...]$  stacking sequence as shown in Table 4 for the quasi-static tests and in Fig. 6 as an example of the dynamic tests. In general, higher percentage of oriented fibers in axial direction (along tube axis), will lead to higher peak load (Hull, 1991), this fact can be used to justify this difference between peak forces.

External chamfer has a significant effect on the peak load, the promising effect of chamfer on the value of peak load that is observed in this work is as peak load of tubes without chamfer > tubes with  $60^\circ$  chamfer > tubes with  $45^\circ$  chamfer. This trend is observed for both static and dynamic crushing tests; Table 4 is presenting peak loads for specimens under static compression.

Because of inertia and possibly strain rate effects on the material properties, the mechanical behavior of CFRPs can be different under different loading rate. There is a noticeable difference between the value of peak load under quasi-static and dynamic crushing in this research where the peak forces in the tests are approximately 1.5 times of those under quasi-static test.

### 3.3 SEA AND AVERAGE CRUSHING FORCE, $F_{ave}$

Both SEA and  $F_{ave}$  can be considered as useful criteria for the energy absorption capacity of an absorber, (Wang, et al., 2016). It was observed in the present study that the values of SEA and  $F_{ave}$  were independent of the chamfer angles. Effects of other investigated parameters on the value of SEA are presented as follows.

The present test results show that the loading rate has a significant effect on the value of SEA as evident in Fig. 7 where the SEA of tested specimens under quasi-static compression and those under dynamic crushing are compared. It seems the brittleness of investigated materials increased with increase in loading rate, thus, specimens under quasi-static have higher values of SEA than those under dynamic impact. Some researchers pointed the strain rate effect and friction as justification for this response (Jackson, et al., 2011).

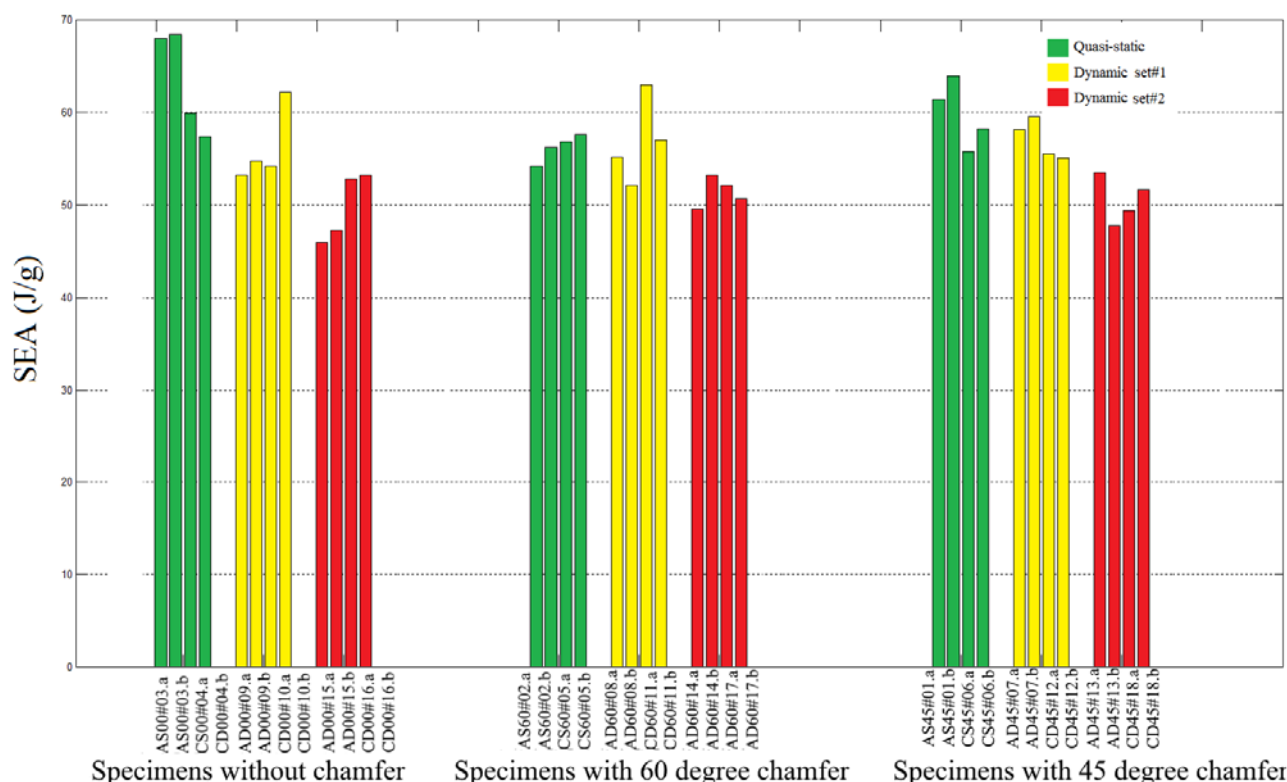


Figure 7. The comparison between SEA value of investigated specimens under quasi-static and dynamic crushing.

In general, SEA of specimens having  $[\pm 45/0\dots]$  stacking sequence is slightly higher than those having  $[0/90\dots]$  stacking sequence. This difference is more significant when the specimens are loaded quasi-statically. The dynamically loaded specimens with  $[\pm 45/0\dots]$  stacking sequence absorbed the same amount of energy with shorter crushed length which shows in comparison tubes having  $[0/90\dots]$  stacking sequence. However, the mass per unit length of tubes with  $[\pm 45/0\dots]$  lay-up is a slightly higher than those of tubes with  $[0/90\dots]$  stack orientation (approximately 5%), therefore, the difference between the value of SEA of different stacking sequences is not obvious as the difference between average crushing load  $F_{ave}$ , ( $SEA = F_{ave}/m_i$ ).

Effect of the striking mass on the value of SEA has not been reported yet, however, results in Fig. 7 show a decrease in the value of SEA with the increase of the striking mass from 102 Kg to 205 Kg (see Fig. 7 and compare the results of dynamic set#1 and set#2). The effect of the initial velocity is often reported in the literature however, the effect of the striking mass has been not explored and it should be further examined.

### 3.4 CRUSH FORCE EFFICIENCY, CE

CE shows deviation of the behavior of an absorber from the behavior of an ideal one ( $CE = F_{ave}/F_{peak}$ ). The higher value of CE (equal to unity) is suitable for crashworthy design (Jones, 1993). External chamfer affects the  $F_{peak}$  and does not affect the  $F_{ave}$ , thus, CE for specimens without chamfer is the lowest and CE for tubes with 45-degree chamfer is the highest (see Table 4 for specimens under quasi-static tests).

### 3.5 CRUSHING MODE

The typical deformation patterns of the crushed zones of specimens with different stacking sequences are completely different, as depicted in Fig. 8. However, the different chamfer angles did not affect the crushing mode of the specimens having the same lay-up orientation. Thus, the ply orientation has a very strong effect on crushing mode while the chamfer angle and dynamic condition had not changed the crushed zone pattern of investigated specimens.

Crushed zone for specimens with  $[0/90\dots]$  stacking sequence can be characterized by long and intact axial splits at the outer layer (oriented along the tube axis) and fragmentation at layers oriented in hoop direction, thus fracture mode for  $[0/90\dots]$  specimens is a combination of 'splaying' and 'fragmentation' which is called 'brittle fracturing'. However, crush zone for tubes with  $[\pm 45/0\dots]$  lay-up is completely different and can be characterized by tearing of plies. In this case it was very difficult to differentiate visually  $\pm 45$  plies from layers in axial direction (0 plies) after impact.

Figure 8 also shows that the loading rate had changed the crushed mode for both investigated lay-up configurations. For instance, crushed zone of specimen with  $[0/90\dots]$  stacking sequence under dynamic impact has several strips at the

outer layer while the internal layers failed by fragmentation mode. The same specimen under quasi static loading has fewer strips at outer layer while the internal layers damaged differently, as it is obvious in Fig 8.c and Fig 8.d. The same finding can be noticed for crushed zone pattern of tubes with  $[\pm 45/0\dots]$  lay-up configuration under dynamic and quasi-static tests.

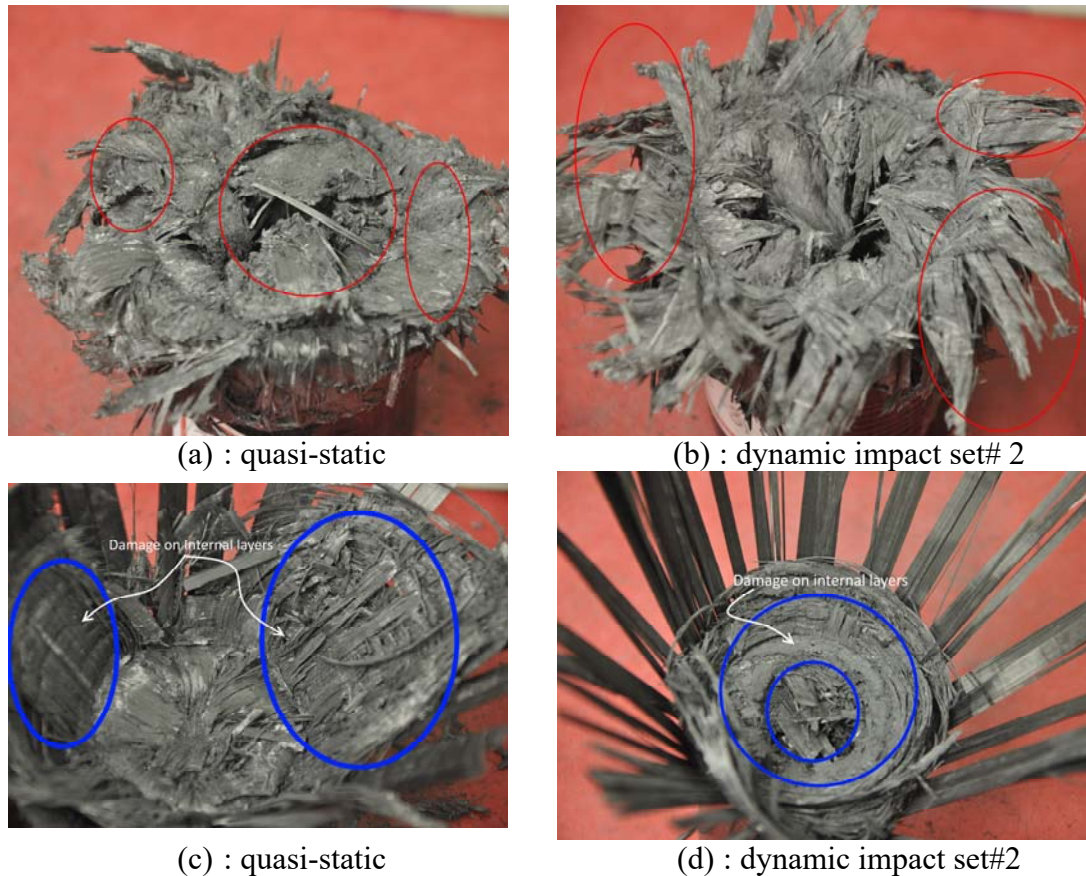


Figure 8. Crush zones of specimens under different loading condition; (a,b) having  $[\pm 45/0\dots]$  stacking sequence; (c,d) having  $[0/90\dots]$  stacking sequence.

#### 4. CONCLUSION

The effects of stacking sequence, loading rate and trigger mechanism on the energy absorption of CF/Epoxy tubes were investigated when analyzing the response of tubes having two different stacking sequences. It was observed in the tests that the stacking sequence controlled the crushing modes of tubes under impact. It was revealed that the mass of the striker has a notable effect on the SEA value so the effect of this loading parameter will be further analyzed. The test results showed that the SEA and average load of tubes under quasi-static loading were higher than those of tubes under dynamic loading as observed in other studies reported in the literature (Schultz and Hyer, 2001; Wang, et al., 2016). This result is in contrast with the dynamic loading effect observed in metal tubes where the SEA and average load usually increase under impact loading. Therefore, the current experimental scheme will be used to perform a further numerical analysis in order to reveal the deformation mechanism that leads to a decrease of the energy absorption capacity of CF/Epoxy tubes under impact loading.

#### 5. REFERENCES

- Bannerman, D. C. and Kindervater, C. M., 1984." Crash Energy Absorption Properties of Composite Structural Elements" In *Proceeding: 4th International SAMPE European Chapter*, Bordeaux, France.
- Chadwick, M. and Caliskan, A., 1997." Crush Mechanisms Observed in Polymeric Composite tubes" *Automotive Composites Consortium Conference*, p. 453-462.
- Fairfull, A.H. and Hull, D., 1987." Effects of Specimen Dimensions on the Specific Energy Absorption of Fiber Composite Tubes". In *Proceeding of ICCM 6*, Edited by F. L. Matthews, N. C. R. Buskell, J. M. Hodgkinson, J. Morton, Elsevier Science and Publishers.

- Farley, G. L., 1983." Energy Absorption of Composite Materials". *Journal of Composite materials.*, Vol. 17, p. 267-279.
- Farley, G. L., 1987." Energy absorption in composite materials for crash worthy structures". In *International Conference of Composite Materials VI*.
- Grundy, J., Blears, J., Sneddon, B.,1985." Assessment of Crash-Worthy Car Materials". *Chartered Mechanical Engineer (CME)*, Vol. 32, p. 31-35.
- Hamouda .M and Sebaey, T.A., 2014." The effect of fiber orientation on the energy absorption capability of axially crushed composite tubes". *Materials & Design*, Vol. 56, p. 923–928.
- Hull, D., 1991." A Unified Approach to Progressive Crushing of Fiber-Reinforced Composite Tubes". *Composites Science and Technology*, Vol. 40, p.377-421.
- Jackson, A., Dutton, S., Gunnion, AJ. and Kelly, D., 2011." Investigation into laminate design of open carbon fibre/epoxy sections by quasi–static and dynamic crushing". *Composite Structure*, Vol.93, p. 2646–54.
- Jones, N. and Wierzbiki, T., 1993. *Structural Crashworthiness and Failure*. Elsevier.
- Mamalis, A. G., Manolacos, D. E., Viegelahn, G. L., Vaxevanidis, N. M. and Johnson, W., 1986." The in extensional collapse of grooved thin-walled cylinders of PVC under axial loading". *International Journal of Impact Engineering*, Vol. 4, p. 41–56.
- Russell, A., Reddy, T., Reid, S. and Soden, P., 1991." Quasi-Static and Dynamic Axial Crushing of Foam-Filled FRP Tubes". *Composite Material Technology, ASME*, Vol. 37, p. 145-152.
- Schultz, M. R., Hyer, M. W. and Fuchs, H. P., 2001." Static and Dynamic Energy-Absorption Capacity of Graphite-Epoxy Tubular Specimens". *Mechanics of Composite Materials and Structures*, Vol. 8, p. 231–247.
- Scueser, D. W and Wickliffe, L. E., 1987." Impact Energy Absorption of Continuous Fiber Composite Tubes". *Journal of Engineering Materials and Technology*, Vol. 109, p. 72-77
- Snowdon, P. and Hull, D., 1984." Energy Absorption of SMC Under Crash Conditions". *International Conference - Fibre Reinforced Composites '84*, p. 1-10.
- Soica, A. and Radu, G. N., 2013. "The influence of triggers geometry upon the stiffness of cylindrical thin walled tubes". *Central European Journal of Engineering*, Vol. 4, p. 101-109.
- Thornton, P.H., 1990." The Crush Behavior of Pultruded Tubes at High Strain Rate", *Journal of Composite Materials.*, Vol. 24, p. 594-615.
- Wade, B., 2014. *Capturing the Energy Absorbing Mechanisms of Composite Structures under Crash Loading*. Ph.D. thesis, University of Washington.
- Wang, Y., Feng, J., Wu, J. and Hu, D., 2016." Effects of fiber orientation and wall thickness on energy absorption characteristics of carbon-reinforced composite tubes under different loading conditions". *Composite Structures*, Vol. 153, p.356–368.

## 6. RESPONSIBILITY NOTICE

The authors are the only responsible for the printed material included in this paper.